Experimental Eye Research 222 (2022) 109168

Contents lists available at ScienceDirect

Experimental Eye Research

journal homepage: www.elsevier.com/locate/yexer

Research article

Preclinical study of a new matrix to help the ocular surface in dry eye disease

Ilenia Abbate [a,*], Cristina Zappulla [a], Manuela Santonocito [a], Santa Viola [a], Luca Rosario La Rosa [a], Giuseppe De Pasquale [a], Elisa Caviola [b], Marisa Meloni [b], Maria Cristina Curatolo [a], Maria Grazia Mazzone [a]

[a] Research, Preclinical Development and Patents, SIFI S.p.A., Lavinaio-Aci S. Antonio, 95025, Catania, Italy
[b] VitroScreen, In Vitro Innovation Center, Milan, 20149, Italy

ARTICLE INFO

Keywords:
Dry eye disease
Tear film homeostasis
Osmoprotectants
Synergistic effect
Matrix
Hyperosmotic stress
Oxidative damage
Ocular surface modulator

ABSTRACT

Dry eye disease (DED), a multifactorial disease of the tears and ocular system, causes loss of tear film homeostasis with damage to the ocular surface. This study aimed to assess whether a peculiar matrix based on sodium hyaluronate (HA), xanthan gum (XNT), glycine (GLY) and betaine (BET) as osmoprotectants, could be involved in biological responses. Wound healing assay on human corneal epithelial (HCE) cells in monolayer showed a synergistic effect of the combination of HA + XNT (**$p \leq 0.01$) together with an efficient extracellular matrix remodeling of the formulation in SkinEthic™ HCE 3D-model sought by integrin beta-1 (ITGβ1) expression and morphological analysis by hematoxylin and eosin (H&E), compared to a reference marketed product. The synergistic effect of HA + XNT + GLY + BET showed an antioxidant effect on HCE cells (***$p \leq 0.001$). Real-time PCR analysis showed that the combination of GLY + BET seemed to ameliorate the effect exhibited by the single osmoprotectants in reducing tumor necrosis factor-alpha (TNFα, #$p \leq 0.05$), interleukin-1 beta (IL1β, ####$p \leq 0.0001$) and cyclooxygenases-2 (COX2, ####$p \leq 0.0001$) genes in SIRC cells under hyperosmotic stress. Furthermore, pretreatment with XNT, alone and in combination (##$p \leq 0.01$), reduced COX2 expression in human non-small cell lung cancer cells (A549). Finally, the formulation was well-tolerated following q.i.d. ocular administration in rabbits during a 28-day study. Due to the synergistic effect of its components, the matrix proved able to repair the ocular surface restoring cell homeostasis and to protect the ocular surface from pro-inflammatory pathways activation and oxidative damage, thus behaving as a reactive oxygen species (ROS) scavenger.

1. Introduction

The ocular surface is characterized by the tear film, a transparent three-layer structure that covers the corneal and conjunctival epithelia ensuring comfort and visual function. The tear film provides nourishment and protects the ocular surface from infections and damage, thus representing the first line of eye defense against pathogenic invasion, and its alteration causes eye discomfort (Pflugfelder and Stern, 2020). Several risk factors, such as old age, female gender, systemic diseases, postmenopausal estrogen treatment, refractive surgery of the cornea, environmental factors and irradiation increase the risk of ocular disease, leading to a considerable impact on patients' quality of life (Smith et al., 2007; Nebbioso et al., 2017; Hu et al., 2021). Recently, some authors surveyed dry eye patients about their unmet needs, and treatment dissatisfaction was found to be the most important aspect to take care of (Asbell et al., 2019; Lee Guo and Akpek, 2020; Okumura et al., 2020).

According to its definition (Craig et al., 2017), Dry Eye Disease (DED) can be described as a disorder that self-sustains, progressively disconnecting from its initial causes. Different factors are described as "entry points" into the vicious circle of DED, in particular tear film imbalance, which is often associated with hyperosmolarity as well as with cellular metabolic disfunction and apoptosis, and the release of pro-inflammatory factors, which causes damage to the ocular surface, with a decrease in goblet cells and loss of corneal epithelial barrier function (Baudouin et al., 2016). The tear film must be constantly replenished by blinking and adequate tear secretion. Without this, the

* Corresponding author. SIFI S.p.A., Via Ercole Patti 36, Lavinaio-Aci S. Antonio, 95025, Catania, Italy.
E-mail address: ilenia.abbate@sifigroup.com (I. Abbate).

https://doi.org/10.1016/j.exer.2022.109168
Received 22 April 2022; Received in revised form 5 June 2022; Accepted 25 June 2022
Available online 28 June 2022

tear film would destabilize and the surface of the eye would be exposed to damaging desiccation and corneal epithelial barrier disruption, leading to eye inflammation, abrasion of the corneal surface, corneal ulcers and vision loss (Bron et al., 2017). Therefore, the therapeutic strategy for DED should consider multiple pathogenic mechanisms.

Nowadays, different artificial tear products are commercially available for the management of dry eye disease. Artificial tears containing viscosity-building macromolecules have been developed, and more recently osmoprotective agents have also been added as compatible solutes to prevent the hyperosmolar tear film from damaging the ocular surface (Simmons and Vehige, 2017; Agarwal et al., 2021). This strategy increases the persistence of the topical product on the ocular surface, and with it its physical protection capacity.

The new formulation analyzed in this study, Hyalistil SYNFO, contains a combination of two macromolecules forming a peculiar matrix of sodium hyaluronate (HA, linear polymer) and xanthan gum (XNT, branched polymer), plus glycine (GLY) and betaine (BET) as osmoprotective agents to improve the cellular homeostasis of the ocular surface. HA, a linear, high-molecular weight glycosaminoglycan polysaccharide, increases the stability of the precorneal tear film, improves ocular surface wettability and smoothness by means of its water-retentive and viscoelastic properties (Khare et al., 2014; Fallacara et al., 2018) and stimulates corneal epithelial cell migration (Gomes et al., 2004), playing a role in wound healing (Litwiniuk et al., 2016). XNT is a high molecular weight anionic polysaccharide capable of forming viscoelastic gels. Its structure contains a pyruvate, which improves its protective effects as antioxidant and scavenger of reactive oxygen species (ROS) (Amico et al., 2015). It is also characterized by lubricating and immunomodulatory properties (Liu et al., 2017), and acts as a scaffold in re-epithelialization processes (Petri, 2015). XNT has recently been shown to improve the conjunctival epithelium of patients with mild to moderate dry eye (Postorino et al., 2020). The interaction of XNT with the mucinous layer of the tear film is sustained through its physicochemical properties and structural characteristics (Menchicchi et al., 2015). Glycine (GLY) and betaine (BET) are compatible solutes useful to stabilize the corneal epithelial cell volume under hyperosmotic stress and to regulate protein function, thus having the potential to manage the effects of tear film instability in DED. Moreover, they play a crucial role in cellular remodeling (Aragona et al., 2013; Chen et al., 2013; Garrett et al., 2013).

Our aim was to investigate the potential synergistic effect of the innovative matrix in the unbalanced and compromised conditions of the ocular surface by means of *in vitro* and *in vivo* efficacy studies.

2. Material and methods

2.1. Materials

Hyaluronic acid was from Shandong TopScience Biotech Co. Ltd. Xanthan gum was from CP Kelco U.S. Inc. (Atlanta, Georgia). Betaine hydrochloride was from Far-malabor S.r.l. (Canosa di Puglia, Italy). Glycine was from Amresco LLC, VWR International (USA). Hyalistil SYNFO was from SIFI S.p.A. (Aci S. Antonio, Catania, Italy). Thealoz Duo was from Thea Laboratoires (France). Immortalized human corneal epithelial cells (HCEs) were obtained from the Riken cell bank (Tsukuba Science City, Japan). SkinEthic™ HCE organotypic corneal 3D tissues and the related maintenance medium were purchased from Episkin Laboratories (Nice, France). Dulbecco's Modified Eagle's Medium (DMEM), phosphate-buffered saline (PBS), glucose oxidase (GOx), human non-small cell lung cancer (A549) cell line, fluorescein sodium salt, 4′,6-diamidino-2′-phenylindole dihydrochloride (DAPI), formalin and hematoxylin were purchased from Sigma-Aldrich S.r.l. (Milan, Italy). Gentamicin, penicillin-streptomycin, L-glutamine (L-glu), trypsin–EDTA, Fetal Bovine Serum (FBS) and Basal Medium Eagle (BME) were from Lonza (Basel, Switzerland). Benzalkonium chloride (BKC) 50% was obtained from Novo Nordisk Pharmatech A/S (Køge, Denmark). Integrin beta-1 (ITGβ1) [4B7R] was purchased from Abcam (Cambridge, UK). AlexaFluor goat anti mouse 488 was from Thermo Fisher Scientific (U.S. Inc.). Eosin and paraffin were purchased from Histoline S.r.l. (Milan, Italy). Lactate dehydrogenase (LDH) cytotoxicity assay kit was obtained from Cayman Chemical (Ann Arbor, Michi-gan). Statens Seruminstitut Rabbit Cornea (SIRC) cells were obtained from LGC Standards S.r.l. (Milan, Italy). RNAlater stabilization solution was obtained from QIAGEN s.r.l. (Milan, Italy). TRIzol reagent, DNase I Amplification Grade, SuperScript II Reverse Transcriptase, Random Hexamer Primer, Oligo(dT)20 primers, dNTP Set 100 mM and SuperScript III Reverse Transcriptase were from Invitrogen by Thermo Fischer Scientific (Carlsbad, CA, USA). TaqMan gene expression assays for tumor necrosis factor-alpha (TNFα), interleukin 1 beta (IL1β), cyclooxygenase-2 (COX2), hypoxanthine phosphoribosyltransferase 1 (HPRT1), glyceraldehyde 3-phosphate dehydrogenase (GAPDH) and real-time PCR master mix were from Applied Biosystems (Foster City, CA, USA). IL1β for the stimulation of A549 cells was from R&D System (Minneapolis, USA). New Zealand White rabbits were purchased from Charles River Laboratories Italia s.r.l. (Lecco, Italy). Tanax® was purchased from MSD Animal Health S.r.l. (Milan, Italy), Zoletil 50 + 50 mg/mL from Virbac (Milan, Italy) and Domitor from Orion Pharma s.r.l. (Milan, Italy).

2.2. In vitro efficacy studies

2.2.1. Wound healing assay

Two different test systems were used for these studies: bidimensional HCE cells in monolayer and SkinEthic™ HCE organotypic 3D tissue constructs.

2.2.1.1. Wound healing assay – HCE cells in monolayer. HCE monolayer was grown in a humidified 5% CO_2 atmosphere at 37 °C in complete culture medium (CCM) made of DMEM containing 10% FBS, 100 units/mL of penicillin-streptomycin and 2 mM of L-glu. Each well of a 48-well tissue culture plate was seeded with 150,000 cells in 400 μL of CCM. Cells were allowed to grow at 37 °C, 5% CO_2 until complete confluence and then subjected to a modified scratch assay protocol (Martinotti and Ranzato, 2020). Briefly, the CCM was removed and wells were washed with phosphate-buffered saline (PBS). Then, cells were incubated for 24 h in DMEM without FBS (FBS-free DMEM) for starvation. Then, the HCE monolayer was scratched with a sterile 200 μL pipette tip, and the cells were washed twice with PBS to remove detached cells prior to incubation with the following treatments: FBS-free DMEM (CTRL−), 0.01% BKC (CTRL +), 0.2% xanthan gum (XNT), 0.2% hyaluronic acid (HA) or with the combination of 0.2% xanthan gum and 0.2% hyaluronic acid (XNT + HA). All test items were diluted in sterile FBS-free DMEM. BKC, was selected as CTRL +, considering that it is the major preservative component currently used in eye drops at concentrations even higher than 0.01% (i.e., 0.02%). Wound closures were observed at T0 and T24 h after scratch under a light microscope (10X, Olympus IX51, Hamburg, Germany). The wound area of each test item at 24 h was compared to the corresponding wound area at T0. Scratch images were acquired by a camera (Olympus DP71, Hamburg, Germany), and areas were analyzed by the ImageJ software (https://imagej.net/Welcome). All samples were tested in three independent experiments performed in triplicate.

2.2.1.2. Wound healing assay - SkinEthic™ HCE organotypic 3D tissue. The wound healing assay performed on SkinEthic™ HCE organotypic 3D tissues was conducted by VitroScreen-In Vitro Research Laboratories (Milan, Italy). The study was performed on triplicate HCE series.

Upon arrival, HCE tissues were aseptically removed from their culture plate, placed in a 6-well culture plate with 1 mL of maintenance medium (changed every 24 h) and incubated overnight at 37 °C, 5% CO_2 saturated humidity. The day after, two parallel injuries were performed on the HCE surface using a glass capillary. One hour after injury, the

HCEs were treated (30 μL) for 24 h or 48 h according to the following treatment groups: i) untreated injured control (Inj Ctrl); ii) Hyalistil SYNFO and iii) Thealoz Duo (as a reference marketed product). On the negative (un-injured and untreated cells) and injured control, 30 μL saline solution (0.9% NaCl) were applied.

Upon treatment completion (24 h and 48 h), tissues were rinsed with saline solution and fixed in formaline. Samples were included in paraffin blocks and sectioned at 5 μm, and ITGβ1 immunostaining was performed. Antibodies: ITGβ1 as primary and AlexaFluor goat anti mouse 488 cell nuclei were stained with DAPI. Images were acquired with LEICA DMi8 THUNDER imager 3D (Leica Microsystem, Wetzler, Germany), camera K5 for fluorescence, and processed with the LASX 3.7.1 software. For each replicate, 2 microscope acquisitions were analyzed at 20x magnification in the injury areas. Image analysis was performed using the LASX 3.7.1 software, in particular the fluorescence signal was quantified considering equal regions of interest (ROIs) comprising the injury and evaluating the % of image area covered by signal, while unspecific signal was removed from the analysis by the software.

Moreover, a histomorphological analysis was performed at 24 h and 48 h by staining tissue sections by hematoxylin and eosin (H&E) staining following an internal method. The stained sections were visualized under a Leica DM 2500 (Leica Microsystem, Wetzler, Germany) bright field microscope equipped with the Leica DFC 450C Camera and LASX 3.0.4 software, for each replicate. Two microscope acquisitions at 40x magnification were analyzed. The overall morphology and its modification were analyzed compared to the untreated injured controls according to defined morphological descriptors: number of cell layers, cell shape (flattened cells during migration or cubic cells in the post-migratory phase) and localization, condensed nuclei for the re-epithelialization process, extra-cellular matrix (ECM) architecture, staining, compactness, cell-cell adhesion and cell-matrix interactions.

2.2.2. Antioxidant effect on HCE cells

HCE cells in monolayer were grown in a humidified 5% CO_2 atmosphere at 37 °C CCM. Each well of a 96-well tissue culture plate was seeded with 60,000 cells per well in 100 μL of CCM. Cells were allowed to grow at 37 °C, 5% CO_2 until subconfluence (70–90%) and subjected to the LDH assay protocol. LDH is a soluble enzyme located in the cytosol that is released into the surrounding culture medium upon cell damage or lysis during apoptosis or necrosis. Therefore, LDH activity in the culture medium can be used as an indicator of cell membrane integrity, and thus as a measure of cytotoxicity: the protocol used is briefly described below (Kaczara et al., 2010; Maugeri et al., 2018). In details, the culture medium was replaced by the following treatments: i) FBS-free DMEM (CTRL−), ii) FBS-free DMEM with GOx (CTRL+), iii) 0.2% XNT, iv) 0.2% XNT + 0.2% HA or with v) 0.2% XNT + 0.2% HA + 0.1% GLY + 0.25% BET (formulation containing the same components of Hyalistil SYNFO). After 3 h, 5 mU/mL of GOx were added to each treatment condition (with exception of CTRL− which remained untreated) for 24 h to induce oxidative stress by continuous mitochondrial H_2O_2 generation. At the end of indicated time point, 100 μL of cell supernatant from each treatment condition were transferred to a new 96-well plate and 100 μL of LDH solution were added to each well. The plate was incubated for 30 min at 37 °C, and then the optical density (O.D.) at 490 nm was read using a spectrophotometer (SPECTRAFluor Plus, Tecan, Männedorf, Switzerland). Cell cytotoxicity percentages were calculated with respect to "spontaneous release" and "maximum release" control wells representing 0 and 100% cytotoxicity levels, respectively. The results were then converted to the corresponding cell viability values. All samples were tested in three independent experiments performed in triplicate.

2.2.3. In vitro model of hyperosmolar stress-induced dry eye in SIRC cells

SIRC cells were grown in a humidified 5% CO_2 atmosphere at 37 °C in a CCM made of BME containing 10% FBS, 100 U/mL of penicillin-streptomycin, 0.1 mg/mL of gentamicin and 2 mM of L-glu. Each well of a 6-well tissue culture plate was seeded with 700,000 cells in 2 mL of CCM, and then confluent cells were subjected to hyperosmolar stress as described below. SIRC cells were switched to FBS-free medium for 24 h, and then treated for 4 h with i) FBS-free isosmolar BME (CTRL−, ≈300 mOsM), ii) hyperosmolar medium (CTRL+, ≈500 mOsM) obtained by addition of sodium chloride (NaCl, 124 mM), iii) 0.1% GLY, iv) 0.25% BET, alone or v) in combination (GLY + BET), all diluted in a hyperosmolar medium. The osmolarity of the culture media was measured by an osmometer (OSMOMAT 010, Gonotec GmbH, Berlin, Germany). After 4 h, the cells were washed with PBS and lysed in TRIzol reagent for RNA extraction. The total RNA (1 μg) was treated with DNase I Amplification Grade to eliminate any potential genomic DNA contamination and reverse-transcribed into cDNA with SuperScript II Reverse Transcriptase and a random hexamer primer. Quantitative real-time PCR (qPCR) was performed in an AbiPrism 7000 thermal cycler (Life Technologies, Modena, Italy) using TaqMan gene expression assays for TNFα (Oc03397715_m1), IL1β (Oc03823250_s1), and COX2 (Oc03398295_m1). The fold change in gene expression was calculated according to the $2^{-\Delta\Delta Ct}$ method (Ct, cycle threshold) using HPRT1 (Oc03399461_m1) as the endogenous reference gene and the average ΔCt of CTRL− as a calibrator. All samples were tested in three independent experiments performed in triplicate.

2.2.4. In vitro model of anti-inflammatory activity in A549 cells

A549 cells were grown in a CCM made of DMEM containing 10% FBS, 2 mM of L-glu and 100 U/mL of penicillin-streptomycin. Each well of a 6-well tissue culture plate was seeded with 200,000 cells in 2 mL of CCM. Cells were allowed to grow at 37 °C and 5% CO_2 until confluence, and then incubated in FBS-free DMEM together with test compounds. Briefly, A549 cells were treated with i) 0.2% XNT, ii) 0.2% HA and iii) 0.2% XNT +0.2% HA for 2 h and then stimulated with 10 ng/ml of IL1β for 18 h to induce COX2 expression. Positive control (CTRL+) is represented by cells exposed to FBS-free DMEM and stimulated with IL1β for 18 h. Subsequently, A549 cells were collected in 1 mL of TRIzol reagent for further RNA isolation following the protocol described above (see section 2.2.3). Quantitative real-time PCR was performed using TaqMan gene expression assays for COX2 (Hs00153133_m1). The fold change in gene expression was calculated according to the $2^{-\Delta\Delta Ct}$ method using GAPDH (Hs02758991_g1) as the endogenous reference gene and the average ΔCt of CTRL− (cells treated with FBS-free DMEM) as a calibrator. All samples were tested in three independent experiments performed in triplicate.

2.3. In vivo study

2.3.1. 28-day ocular tolerability study in rabbits

Ten New Zealand White (NZW) rabbits, 5 males and 5 females, weighing approximately 2 Kg, were used in this study. All animals were treated according to the Directive 2010/63/UE, the European Convention for the Protection of Vertebrate Animals used for Experimental and Other Scientific Purposes and to the Association for Research in Vision and Ophthalmology (ARVO) Statement for the Use of Animals in Ophthalmic and Vision Research. Protocols were approved by the Italian Ministry of Health (authorization no. 672/2016-PR of 05 April 2016). All animals were housed individually in standard cages under identical temperature (18–23 °C), relative humidity (45–65%) and controlled enrichment conditions, and exposed to a 12-h light and darkness cycle. In order to mimic the human dosing regimen, 50 μL of Hyalistil SYNFO formulation or control [phosphate-buffered saline (PBS)] were administered four times a day (*q.i.d.*), every 3 h for 28 days by instillation into the conjunctival sac of the right (treated) or left (control) eye, respectively. The general clinical signs of all animals, such as body weight (BW) and general appearance, were observed and recorded following the schedule summarized in Table 1. Two types of ocular examinations were conducted for clinical evaluations using an ophthalmoscope and a slit lamp, as reported in Table 1.

Table 1
Schedule of procedures, ocular examinations and sampling.

Study time points	Procedure	Ocular examination
Baseline	General clinical examination BW	Slit lamp Observation with an ophthalmoscope
Day 1	General clinical examination Instillations	Observation with an ophthalmoscope after the second and the last administration of the day (+1h ± 6 min after the second and the fourth administration)
Day 2 to Day 28	General clinical examination (daily) BW (weekly) Instillations (daily)	Slit lamp before the first administration of the day (weekly) Observation with an ophthalmoscope before the first administration of the day (weekly)
Day 29	General clinical examination BW Euthanasia	Slit lamp Observation with an ophthalmoscope

The potential ocular irritancy and/or damaging effects of the formulation were evaluated according to a modified Draize's test (Draize et al., 1944). Redness (A), swelling (B) and discharge (C) of the conjunctiva, evaluated with an ophthalmoscope, were graded on a scale from 0 to 3, 0 to 4 and 0 to 3, respectively. The maximum total score was 20, calculated as follow: Score (A + B + C) x 2. Moreover, slit lamp examinations of both eyes were performed to assess corneal area, corneal epithelial staining and iris hyperemia (score 0 to 4), according to the McDonald–Shadduck's scale (Baldwin et al., 1973; McDonald and Shadduck, 1977). Fluorescein sodium salt 1% staining was used to evaluate corneal integrity, as it allows accurate determination of the extent of epithelial damage because of its poor diffusion through the stromal layer of the cornea.

At the end of the experiment, the animals were euthanized by an intravenous injection of 500 μL/kg of Tanax following sedation with a mixture of 100 μL/kg of Zoletil and 100 μL/kg of Domitor.

2.4. Statistical analysis

On HCE monolayers, significant differences were sought by one-way ANOVA, followed by Sidak's or Tukey's post-hoc tests (GraphPad Prism 6; CA, USA) for the wound-healing and antioxidant assays, respectively. P values ≤ 0.05 were considered statistically significant.

On SkinEthic™ HCE 3D tissue, the statistical analysis of ITGβ1 protein expression was performed by one-way ANOVA followed by Tukey's post-hoc test (GraphPad Prism 9; CA, USA).

Differences among treatments in the hyperosmolarity dry eye model and anti-inflammatory assay were sought by one-way ANOVA, followed by Sidak's post-hoc test (GraphPad Prism 6; CA, USA).

In the 28-day ocular tolerability study, statistically significant differences were sought by an ANOVA General Linear Model test (Minitab 17 software, Coventry, United Kingdom).

3. Results

3.1. Wound healing effect – HCE cells in monolayer

HCE cells in monolayer were subjected to scratch assay and treated with 0.2% xanthan gum (XNT), 0.2% hyaluronic acid (HA) or with their combination (XNT + HA). The analysis of HCE monolayer scratch areas showed that benzalkonium chloride (BKC) 0.01% (CTRL+) is unable to induce re-epithelialization (Fig. 1). 0.2% XNT and 0.2% HA, when used alone, failed to reach statistical significance at 24 h with respect to the CTRL− condition. The combination of XNT + HA showed a statistically relevant re-epithelialization effect vs CTRL− ($**p \leq 0.01$) and a synergistic effect vs the single components ($\#p \leq 0.05$), which supports the synergistic effect of 0.2% XNT with 0.2% HA (Fig. 1).

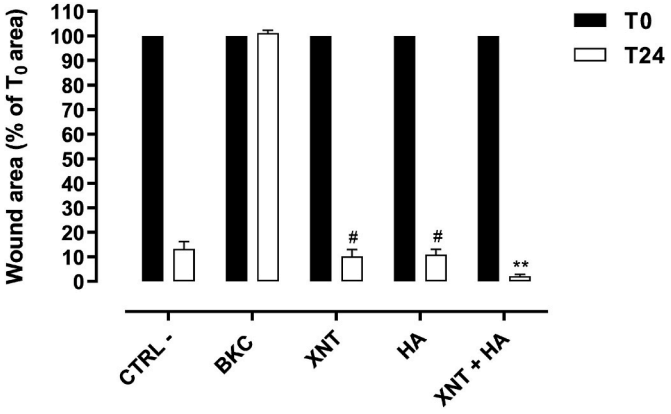

Fig. 1. Wound healing in HCE monolayer. HCE cells were exposed for 24 h to FBS-free DMEM (CTRL−), benzalkonium chloride 0.01% (BKC, CTRL+), 0.2% xanthan gum (XNT), 0.2% hyaluronic acid (HA) and 0.2% XNT + 0.2% HA (XNT + HA). Data are presented as mean ± S.E.M. of three independent experiments performed in triplicate. $**p \leq 0.01$ vs. CTRL−; $\#p \leq 0.05$ vs. XNT + HA. One-way ANOVA followed by Sidak's post-hoc test.

3.2. Wound healing effect - SkinEthic™ HCE organotypic 3D tissue

The efficacy of Hyalistil SYNFO on boosting or accelerating re-epithelialization was evaluated in an experimental window of 24 h–48 h on SkinEthic™ HCE organotypic 3D tissue addressing: i) expression of integrin beta-1 (ITGβ1) by immunofluorescence and ii) tissue morphology by hematoxylin and eosin (H&E) staining at the site of superficial injuries, where a more relevant cellular activity was detected.

In untreated injured control, (Inj Ctrl) ITGβ1 was found to be expressed and localized in the early migratory phase at 24 h and to decrease at 48 h, when it was no longer detectable (Fig. 2 A–B; Fig. 3 A–B). In the experimental window relevant for the migratory phase (i.e., 24 h–48 h), the test items have determined a different ITGβ1 modulation and kinetic. In detail, in Hyalistil SYNFO treated samples, protein expression was found at the migratory edges at 24 h (Fig. 2 A; Fig. 3 A) and was no longer detected at 48 h (Fig. 2 B; Fig. 3 B). On the other hand, in ThealozDuo treated samples, ITGβ1 was not detected at 24 h ($**p \leq 0.01$ vs. Inj Ctrl, Fig. 2 A and Fig. 3 A) and its expression started at 48 h (Fig. 2 B and Fig. 3 B), showing a delay in the re-epithelialization process compared to Hyalistil SYNFO.

Tissue morphology was evaluated by H&E staining with the aim of investigating the modification in the HCE tissue structure during wound healing by analyzing the morphological descriptors involved in re-epithelialization (24 h) and re-modelling (48 h).

Morphological analysis by H&E at 24 h showed that cell migration and proliferation (red rectangle) processes were similar in the untreated injured control (Inj Ctrl) and in the Hyalistil SYNFO series (Fig. 4 A), suggesting that the physiological re-epithelialization process, as response to the injury, occurred with the same kinetics. Interestingly, tissue architecture was better organized in the Hyalistil SYNFO-treated group compared to Inj Ctrl (Fig. 4 A), the former presenting a lower number of condensed nuclei (black arrows). Overall tissue organization seems to be recovered, resulting in a more regular HCE morphology. Moreover, the cells treated with Hyalistil SYNFO were also characterized by a smoother corneal surface and conserved epithelial continuity. On the contrary, the morphological analysis on ThealozDuo-treated HCEs showed presence of elongated cells that are still in a migratory phase around and below the injury site (Fig. 4 A).

The morphological descriptors of re-modelling, related to epithelial extracellular matrix (ECM), cellular spatial disposition and adhesion

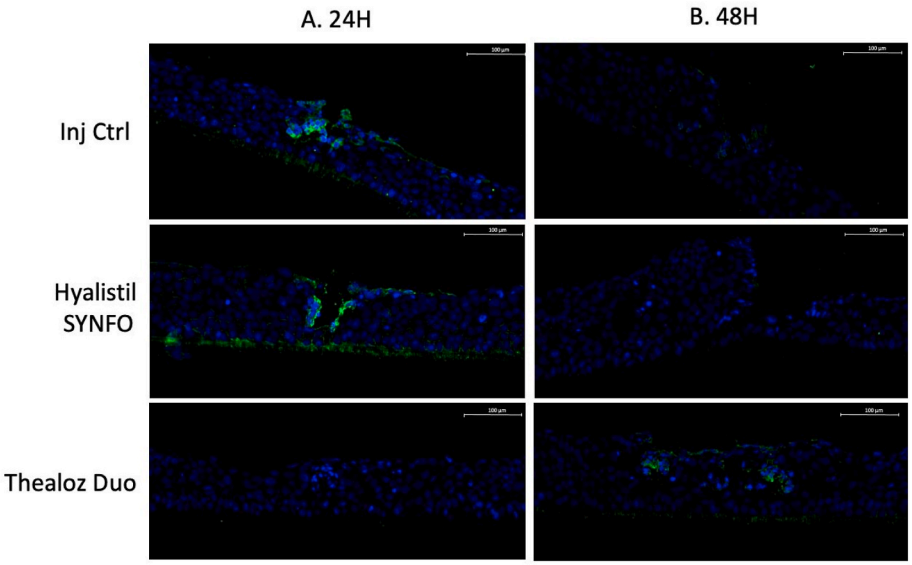

Fig. 2. ITGβ1 immunofluorescence staining at 20x magnification. Representative pictures of the injury site of SkinEthic™ HCE organotypic 3D tissue at 24 h (A) and 48 h (B) treated with the following test items: untreated injured control (Inj Ctrl), Hyalistil SYNFO and Thealoz Duo. ITGβ1 (green), DAPI (blue). Scale bar: 100 μm.

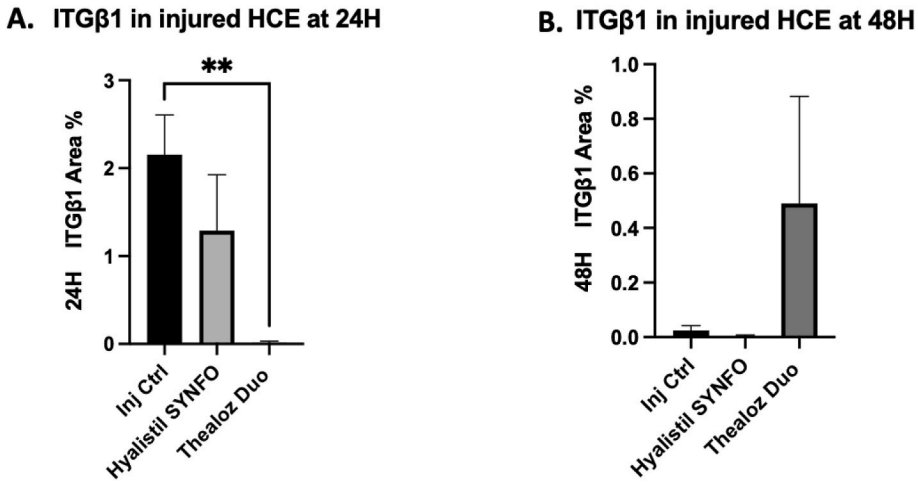

Fig. 3. ITGβ1 protein quantification at the injury site in SkinEthic™ HCE organotypic 3D tissue treated for 24 h (A) and 48 h (B) with the following test items: untreated injured control (Inj Ctrl), Hyalistil SYNFO and Thealoz Duo. Data are expressed as the % of area covered by fluorescent signal, measured in a selected region of interest (ROI) comprising the injury. Data are presented as mean ± standard deviation of biological triplicates. $^{**}p \leq 0.01$ vs. Inj Ctrl; One-way ANOVA followed by Tukey's post-hoc test.

were also evaluated at 48 h (Fig. 4 B). In Inj Ctrl HCEs, in proximity of the injury (green ellipse), the ECM matrix architecture was disorganized with irregular cell-cell contacts, and many condensed nuclei were found (Fig. 4 B). In the Hyalistil SYNFO-treated HCE tissue, the HCE architecture was almost recovered, showing regular cell-cell contacts within the different layers, round shape cells without vacuolization and a quite homogeneous ECM organization (Fig. 4 B). Finally, in Thealoz Duo-treated samples, the whole tissue morphology and architecture were improved compared to untreated injured control, with a reduction of vacuolization and an increase of cellular connection, although the HCE tissue still appears not fully recovered and ECM results not completely homogeneous (Fig. 4 B).

3.3. Antioxidant effect on HCE cells

Oxidative stress was induced by the glucose oxidase enzyme (GOx), and the antioxidant effect, in terms of cell viability, was evaluated by LDH assay. Indeed, while ROS determination represents a direct measure of the antioxidant effect, cell viability can be considered an indirect indicator of oxidative stress. Results showed that, after the stress induced by GOx, both 0.2% XNT alone and the combination of 0.2% XNT and 0.2% HA (XNT + HA) increased cell viability compared to the positive control (CTRL+, $^{**}p \leq 0.01$) (Fig. 5). Interestingly, when both polymers are mixed with osmoprotectants (XNT + HA + GLY + BET) the synergistic effect is more evident, showing an increase in cell viability (Fig. 5). Indeed, XNT + HA + GLY + BET increases cell viability in a statistically significant manner compared to CTRL− ($^{***}p \leq 0.001$) and *versus* XNT and XNT + HA ($\#\#p \leq 0.01$), respectively (Fig. 5).

3.4. Effect of osmoprotectants on the hyperosmolar stress in SIRC cells

SIRC cells were exposed to hyperosmolar stress using NaCl 500 mOsm and treated with GLY and BET as single osmoprotectants or with a combination of both (GLY + BET) for 4 h to simulate *in vitro* dry eye.

Evaluations carried out by qPCR demonstrated that the expression of the TNFα ($^{**}p \leq 0.01$), IL1β ($^{****}p \leq 0.0001$) and COX2 ($^{****}p \leq 0.0001$) pro-inflammatory genes was significantly upregulated in cells grown in a hyperosmolar medium (CTRL+) in the absence of osmoprotectants compared to the negative control (CTRL−) (Fig. 6A–C).

The treatment of SIRC cells with the single osmoprotectants GLY and BET significantly reduced the expression of TNFα by 70% ($\#p \leq 0.05$) and 73.6% ($\#p \leq 0.05$), respectively and of IL1β by 61.8% ($\#\#\#p \leq$

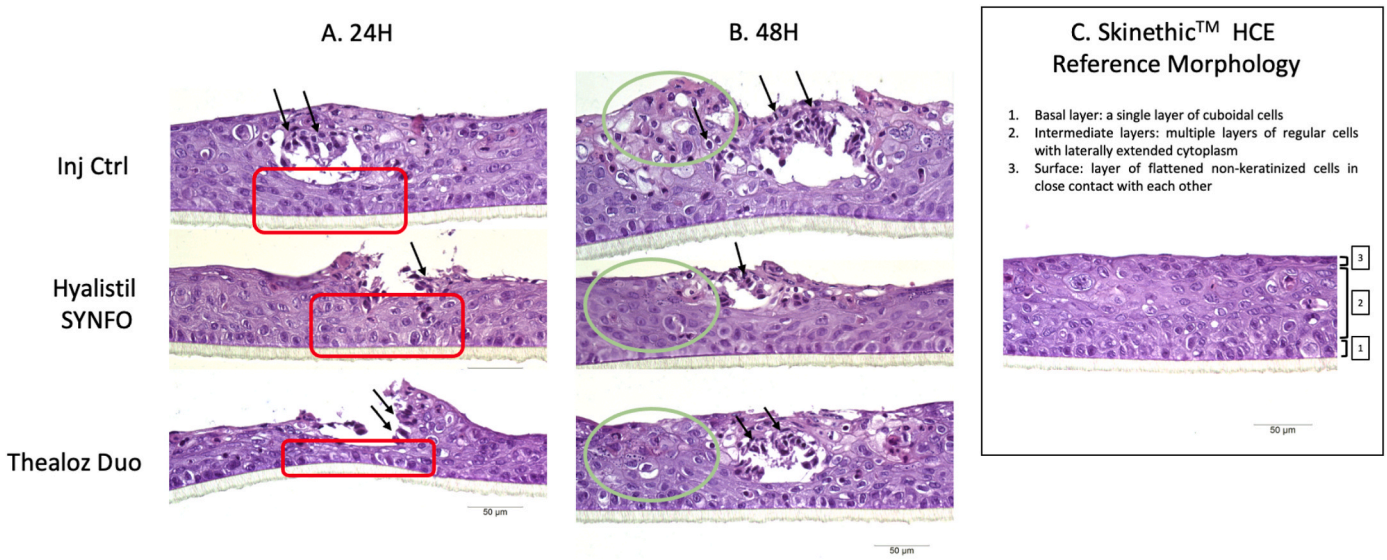

Fig. 4. Morphological analysis by H&E staining at 40x magnification. Representative pictures of the injury site in SkinEthic™ HCE organotypic 3D tissue treated for 24 h (A) and 48 h (B) with the following test items: untreated injured control (Inj Ctrl), Hyalistil SYNFO and Thealoz Duo. Morphological descriptors were evaluated in relevant areas for re-epithelialization at 24 h (red rectangles) and re-modelling at 48 h (green ellipse) as well as condensed nuclei (black arrows). Standard Morphology of Skinethic™ HCEs was reported as reference (C). Scale bar: 50 µm.

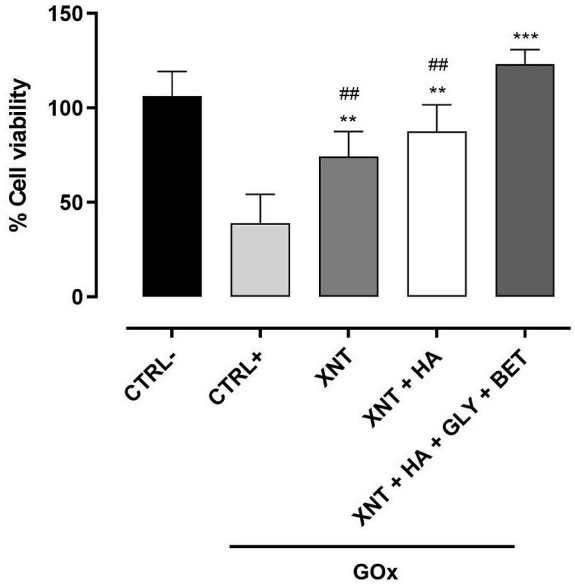

Fig. 5. Antioxidant effect, in terms of cell viability (LDH assay), of 0.2% XNT (XNT) alone or in combination with 0.2% hyaluronic acid (XNT + HA) and 0.1% glycine and 0.25% betaine as osmoprotectants (XNT + HA + GLY + BET) on HCE cells induced with GOx (5mU/mL). $^{**}p \leq 0.01$, $^{***}p \leq 0.001$ vs. CTRL+. $\#\#p \leq 0.01$ vs. XNT + HA + GLY + BET. Two-way ANOVA followed by Tukey's post-hoc test. Data represent the mean ± S.E.M. of 3 different experiments performed in triplicate.

0.001) and 76.2% ($\#\#\#p \leq 0.001$), respectively compared to CTRL+ (Fig. 6A and B). In addition, BET was also able to reduce ($\#\#\#\#p \leq 0.0001$) the expression of COX2 mRNA significantly by 64.7% compared to CTRL+ (Fig. 6 C). Interestingly, when SIRC cells were treated with the combination of both osmoprotectants, GLY + BET seemed to ameliorate the effect exhibited by the single components reducing the expression of all pro-inflammatory genes, even if it failed to reach statistical significance (Fig. 6A–C).

3.5. Anti-inflammatory activity on A549 cells

A549 cells were treated with 0.2% XNT (XNT), 0.2% HA (HA) and with their combination (XNT + HA) for 2 h and then stimulated with 10 ng/mL of IL1β for 18 h to induce COX2 expression.

Quantitative real-time PCR analysis showed that stimulation of A549 cells with IL1β (CTRL + IL1β) produced a statistically significant overexpression of the COX2 mRNA level to 9.44-fold ($^{****}p \leq 0.0001$) compared with CTRL− (Fig. 7). The expression of COX2 in response to IL1β stimulation was significantly reduced by 6-fold ($\#\#p \leq 0.01$) by pretreating cells with XNT or XNT + HA compared with CTRL+, showing an effect in preventing inflammation. However, this effect seems to be ascribable to XNT alone rather than to a synergy of both polymers. Moreover, it was found that 0.2% HA was statistically different compared to 0.2% XNT alone and the combination XNT + HA ($p \leq 0.001$ vs 0.2% HA) (Fig. 7).

3.6. 28-day ocular tolerability study in rabbits

Ocular tolerability of Hyalistil SYNFO was evaluated following unilateral instillation of 50 µL *q.i.d.* into the eyes of NZW rabbits for 28 days.

Redness (A), swelling (B), and discharge (C) of the conjunctiva were evaluated for both eyes using an ophthalmoscope according to the Draize's scale. The results of the ophthalmoscopic assessments after treatment with Hyalistil SYNFO did not reveal any major findings throughout the experiment. Indeed, treatment with Hyalistil SYNFO only produced sporadic and sparse events of transient and low-score conjunctival redness, i.e., a maximum score of 1 on a scale from 0 to 20. There was no statistically significant difference between male and female rabbits, nor between right eyes treated with Hyalistil SYNFO and left eyes treated with the control (PBS) (Fig. 8). The resulting score remained extremely low during the whole study.

Examination of the ocular surface, particularly of corneal area, corneal epithelial staining and iris hyperemia was performed with a slit lamp. Analysis of data by means of the McDonald-Shadduck's scale showed no persisting or relevant ocular findings during the whole study in both treated (Hyalistil SYNFO) and contralateral eyes (PBS). Here we report a representative graph of the corneal epithelial staining (Fig. 9). Slit lamp examination also demonstrated that treatments with both Hyalistil SYNFO and PBS only produced a slight and transient

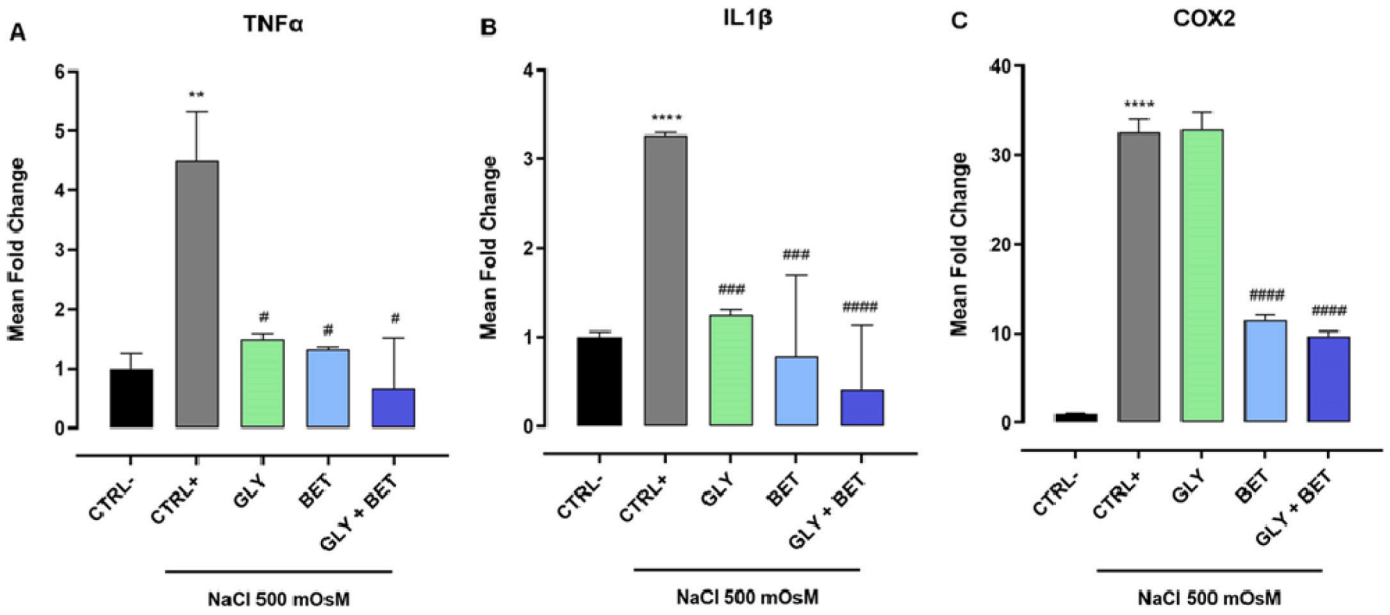

Fig. 6. Quantitative real-time PCR gene expression profile of pro-inflammatory mediators: (A) tumor necrosis factor-alpha (TNFα); (B) interleukin 1 beta (IL1β); (C) cyclooxygenase-2 (COX2) in Statens Seruminstitut Rabbit Cornea (SIRC) cells. SIRC cells were exposed for 4 h to i) FBS-free isosmolar medium (CTRL−, ≈300 mOsM), ii) hyperosmolar medium (CTRL+, ≈500 mOsM) made of sodium chloride (NaCl, 124 mM), iii) 0.1% glycine (GLY), iv) 0.25% betaine (BET) alone or v) in combination (GLY + BET), all diluted in a hyperosmolar medium. #$p \leq 0.05$, ###$p \leq 0.001$ and ####$p \leq 0.0001$ vs. CTRL+. **$p \leq 0.01$ and ****$p \leq 0.0001$ vs. CTRL−. One-way ANOVA followed by Sidak's post-hoc test.

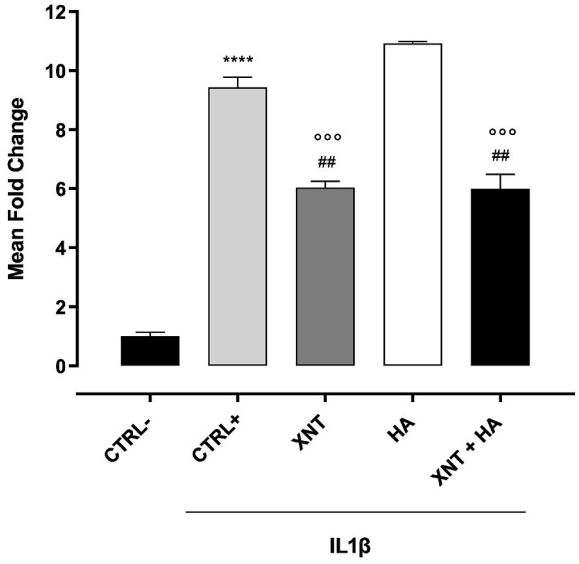

Fig. 7. Quantitative real-time PCR gene expression profile of the pro-inflammatory mediator cyclooxygenase-2 (COX2) in human pulmonary adenocarcinoma (A549) cells. A549 cells were exposed for 2 h to 0.2% xanthan (XNT), 0.2% hyaluronic acid (HA) and to a combination of 0.2% XNT + 0.2% HA (XNT + HA) and then stimulated with 10 ng/mL of IL1β for 18 h. Cells exposed to FBS-free DMEM and stimulated with IL1β for 18 h in the absence of treatment represent the positive control (CTRL+). ##$p \leq 0.01$ vs. CTRL+. ****$p \leq 0.0001$ vs. CTRL−. p ≤ 0.001 vs 0.2% HA. One-way ANOVA followed by Sidak's post-hoc test.

fluorescein staining of the cornea confined to a small focus (score of 1 on a scale from 0 to 4 for both for the epithelial staining and the corneal area), similarly toPBS control eyes (Fig. 9). Statistical analysis showed no significant difference between male and female rabbits, nor between right eyes treated with Hyalistil SYNFO and left eyes treated with PBS. Under these experimental conditions, these results demonstrate that

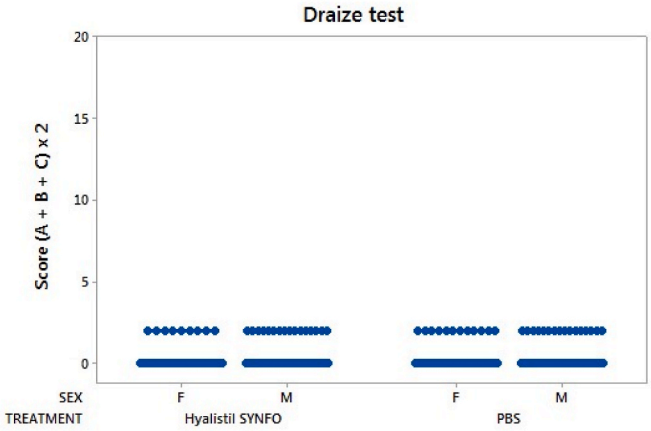

Fig. 8. Draize test scores for female and male rabbits and for the different treatments: right eye treated with Hyalistil SYNFO and left eye treated with the control (PBS) over 28 days in the ocular tolerability study.

Hyalistil SYNFO administrated four times a day for 28 days is well tolerated, as is PBS.

4. Discussion

DED is an underdiagnosed and undertreated disease that occurs as part of ageing and impacts the quality of life of millions of affected individuals worldwide. The numbers of DED patients have dramatically increased in the past decades (up to 30–40% in some populations), which is likely to be predominantly caused by environmental changes (Tsubota et al., 2020).

The core mechanism of DED is evaporation-induced tear hyperosmolarity, which is the hallmark of the disease. It damages the ocular surface both directly and by initiating inflammation. In DED, tear hyperosmolarity is considered to be the trigger for a cascade of signaling events within surface epithelial cells, which leads to the release of

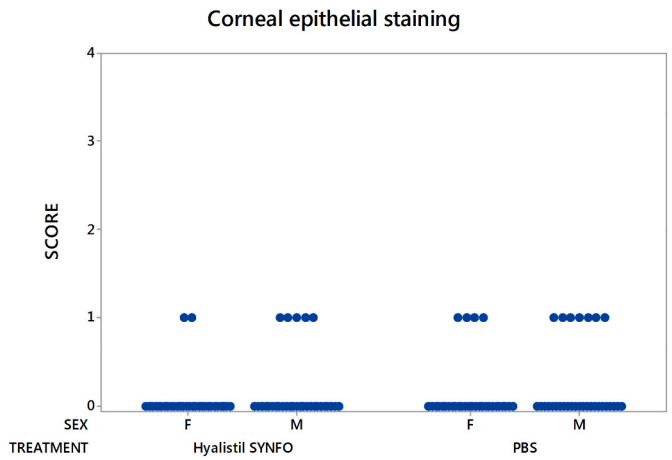

Fig. 9. Corneal staining scores by means of the McDonald-Shadduck's scale for female and male rabbits and for the different treatments: right eye treated with Hyalistil SYNFO and left eye treated with the control (PBS) over 28 days in the ocular tolerability study.

inflammatory mediators and proteases. The net result is the characteristic punctate epitheliopathy of DED and a tear film instability which leads at some point to early tear film breakup. This breakup exacerbates and amplifies tear hyperosmolarity and completes the vicious circle events that lead to ocular surface damage. Ultimately this is thought to lead to self-perpetuation of the disease (Craig et al., 2017). As a multifactorial disease, dry eye presents with a wide spectrum of ocular surface alterations that have various etiologies, as well as with many different clinical and symptomatic manifestations that are difficult to address with a single diagnostic test or course of treatments (Barabino et al., 2021). Artificial tears are the mainstay of therapy for the treatment of DED. Only a few drugs are approved for DED-related inflammation, but given the heterogeneous nature of the disease and the limitations of current treatments, there is a growing demand for new therapeutic strategies that address the considerable unmet needs of the market (Gupta et al., 2020). Recently, a group of experts has proposed a new terminology for DED and, using a consensus-based method called nominal group technique (NGT), they attempted to classify eye drops in wetting agents, multiple-action tear substitutes and ocular surface modulators (Barabino et al., 2020). In particular, Barabino et al. asserted that an ideal therapeutic strategy should simultaneously restore the loss of homeostasis of the ocular surface, blocking the vicious circle of chronic inflammation and ocular damage.

Therefore, a peculiar new matrix named Hyalistil SYNFO, based on a combination of two macromolecules, a linear polymer (sodium hyaluronate) and a branched one (xanthan gum), with the addition of osmoprotectants (glycine and betaine) was designed and developed. On this premise, the efficacy of the matrix was evaluated by means of validated *in vitro* assays widely used to test re-epithelialization, regulation of osmolarity, prevention of inflammation and antioxidant activity. Moreover, the ocular safety of Hyalistil SYNFO was evaluated in a 28-day ocular tolerability study in rabbits.

Firstly, the effect of HA and XNT, alone or in combination (XNT + HA), was investigated in corneal wound healing, a well-known physiological process divided into a sequence of events that can be summarized in three main phases: i) lag phase, ii) migration/re-epithelialization, iii) proliferation, stratification, and differentiation (Liu and Kao, 2015). During re-epithelialization, the epithelial cells adjacent to the injury flatten and migrate to seal the margins of the wound; then, a first cell proliferation process is initiated to increase tissue thickness and re-establish the integrity of the corneal epithelium. In the *in vitro* scratch assay with HCE cell monolayers, the results demonstrated that, when used alone, XNT and HA failed to reach statistical significance at 24 h respect to negative control, but a relevant statistically difference was obtained versus HA + XNT ($\#p \leq 0.05$). Therefore polymers, which have no effect on the physiological tissue repair process when tested individually, showed a synergistic effect on re-epithelialization when mixed together.

In the re-epithelialization process, a pivotal role is played by integrins, membrane proteins involved in cell-to-cell, cell-to-ECM anchoring. In physiological and homeostatic conditions, integrin β1 is only expressed in the basal layer of the corneal epithelium (McKay et al., 2020), while in wounded tissues it is detected along the cell membrane at the edges of the injury as a consequence of the activation of the wound healing process based on cytoskeleton re-organization, to promote cell migration. An early expression of the protein therefore favors the establishment of a fast migration front and efficient re-epithelialization. In cells located on the edge of the injury, integrins are dissociated from the hemidesmosomes and desmosomes and distributed on the cellular surface of the migratory front, offering points for cell migration and anchorage for the apposition of fibers and matrix proteins (Carter, 2009). During the subsequent re-modelling process, the re-organization of ECM and cell-to cell junctions allows the restoration of the cornea architecture. On these premises, ITGβ1 expression and localization were investigated by immunofluorescence and morphological modifications by H&E analysis in a corneal wound healing model. Using a SkinEthic™ HCE 3D-model, the effect of Hyalistil SYNFO was observed within an experimental window chosen to recapitulate the migratory phase (24 h post injury) and epithelial ECM remodeling (48 h post injury) compared to Thealoz Duo, a marketed reference product. It was found that the Hyalistil SYNFO mimics the timing of the physiological corneal re-epithelialization process and accelerates the proliferative phase, resulting in a more regular organization of cell layers and tissue architecture. On the contrary, Thealoz Duo shows a different action on the ITGβ1 protein characterized by a delayed kinetic of expression (no detection at 24 h and modulation at 48 h), despite promoting a good quality of the tissue compared to Inj Ctrl at 48 h. These results are also supported by the H&E morphology analysis, which suggest that Hyalistil SYNFO allows the physiological process of re-epithelialization by promoting a conserved and regular re-organization of the tissue architecture. Overall, these data suggest a difference in the mechanism of action of the two ophthalmic formulations, in particular: Hyalistil SYNFO is shorter acting (i.e., at 24 h) and reproduces the physiological process of re-epithelialization, while Thealoz Duo induces ITGβ1 expression with a delayed kinetic at 48 h. Moreover, each single component of the innovative matrix, based on their peculiar properties, contributes to favoring a more rapid re-epithelialization. In particular, the synergy of the two polymers accelerated cell proliferation, whereas osmoprotectants have shown early efficacy in pushing the migratory phase and anticipating tissue remodeling (Supplementary data Figs. 1 and 2).

Considering the central role of ROS in propagating the dry eye cycle (Seen and Tong, 2018), the antioxidant properties of the components of this peculiar matrix were investigated, alone and mixed together, in an *in vitro* model of HCE cells stressed with the GOx enzyme. The results showed a combined action of 0.2% HA and 0.2% XNT. It is also noteworthy that this synergistic effect on the oxidative stress is more evident when both polymers are mixed with GLY and BET as osmoprotectants.

Tear film osmolarity is an important causative factor in the pathogenesis of DED. Tear hyperosmolarity resulting from decreased lacrimal flow contributes to ocular surface damage through a cascade of inflammatory events (Baudouin et al., 2016; Craig et al., 2017). Therefore, the osmoprotective effect of GLY and BET was assessed on the expression of three key inflammatory mediators (i.e., TNFα, IL1β and COX2) in SIRC cells exposed to hyperosmolar stress. Notably, the combination of the two osmoprotectants (GLY + BET) seemed to exhibit improved efficacy in reducing the expression of pro-inflammatory genes involved in hyperosmolar stress compared to the same single osmoprotectants or other osmoprotectants tested. In light of the crucial role of inflammation in the dry eye vicious circle (Menchicchi et al., 2015; Gupta et al., 2020; Tsubota et al., 2020; Rolando and Barabino, 2021), the effect of both

polymers XNT and HA, alone or in combination, in preventing inflammation was assessed using an *in vitro* model of A549 cells stimulated with IL1β. Importantly, the pre-treatment of A549 cells with XNT prior to the inflammatory stimulus with IL1β was able to reduce COX2 mRNA expression both when tested alone and in association with HA.

Finally, the Hyalistil SYNFO formulation also showed a good tolerability profile in NZW rabbits during a 28-day ocular tolerance study. No relevant ocular pathological findings were recorded following *q.i.d.* ocular topical administration for up to 28 days.

Therefore, according to the results obtained and based on an updated tear substitute classification and considering the advantages provided by *in vitro* models (Barabino et al., 2020), the new product Hyalistil SYNFO could be classified as "ocular surface modulator" referring to polymers or combination of molecules with scientifically demonstrated capability to interact with and to influence the ocular surface components, with particular regard to the epithelial cells, promoting homeostasis and cellular well-functioning.

5. Conclusion

Altogether, these data suggest that the peculiar new matrix Hyalistil SYNFO has re-epithelializing and antioxidant activity, regulates osmolarity and prevents inflammation, besides having a good impact in terms of safety, warranting further clinical evaluation.

As a result of a combination of sodium hyaluronate, xanthan gum and osmoprotectants, Hyalistil SYNFO may be able to hydrate, lubricate and contribute to repair the ocular surface imbalance in DED. Moreover, it contributes to restoring cell homeostasis and protecting the ocular surface from oxidative damage, thus behaving as a scavenger of ROS and eventually modulating the inflammatory process.

Declaration of interest

Ilenia Abbate, Cristina Zappulla, Manuela Santonocito, Santa Viola, Luca Rosario La Rosa, Maria Cristina Curatolo and Maria Grazia Mazzone are coinventors of the international patent "Ophthalmic composition and use thereof in the treatment of eye diseases". Publication Number WO2021260622A1. Publication Date 30 December 2021. International Application No. PCT/IB 2021/055617. International Filing Date 24 June 2021.

Ilenia Abbate, Cristina Zappulla, Manuela Santonocito, Santa Viola, Luca Rosario La Rosa, Giuseppe De Pasquale, Maria Cristina Curatolo and Maria Grazia Mazzone are all employees at SIFI S.p.A. Elisa Caviola and Marisa Meloni declare no conflict of interest.

Financial Support

This research did not receive any specific grant from funding agencies in the public, commercial, or not-for-profit sectors.

Acknowledgments

The authors kindly thank Francesco Cuffari, Angelo Pricoco, Donato Spina, Veronica Pepe and Carmela Giovanna Spoto for their technical support in the production and characterization of lab-scale formulation batches used in the studies, Pasqualino Giuffrida for taking care of SIFI's animal house. We also thank Elena Solfato and Francesco Giuliano for their scientific support.

Appendix A. Supplementary data

Supplementary data to this article can be found online at https://doi.org/10.1016/j.exer.2022.109168.

References

Agarwal, P., Craig, J.P., Rupenthal, I.D., 2021. Formulation considerations for the management of dry eye disease. Pharmaceutics 2, 207. https://doi.org/10.3390/pharmaceutics13020207.

Amico, C., Tornetta, T., Scifo, C., Blanco, A.R., 2015. Antioxidant effect of 0.2% xanthan gum in ocular surface corneal epithelial cells. Curr. Eye Res. 1, 72–76. https://doi.org/10.3109/02713683.2014.914542.

Aragona, P., Rania, L., Roszkowska, A.M., Spinella, R., Postorino, E., Puzzolo, D., Micali, A., 2013. Effects of amino acids enriched tears substitutes on the cornea of patients with dysfunctional tear syndrome. Acta Ophthalmol. 6, 437–444. https://doi.org/10.1111/aos.12134.

Asbell, P., Messmer, E., Chan, C., Johnson, G., Sloesen, B., Cook, N., 2019. Defining the needs and preferences of patients with dry eye disease. BMJ Open Ophthalmol. 1, e000315 https://doi.org/10.1136/bmjophth-2019-000315.

Baldwin, H.A., McDonald, T.O., Beasley, C.H., 1973. Slit-lamp examination of experimental eyes. II. Grading scales and photographic evaluation of induced pathological conditions. J. Soc. Cosmet. Chem. 24, 181–195.

Barabino, S., Aragona, P., di Zazzo, A., Rolando, M., 2021. Updated definition and classification of dry eye disease: renewed proposals using the nominal group and Delphi techniques. Eur. J. Ophthalmol. 1, 42–48. https://doi.org/10.1177/1120672120960586.

Barabino, S., Benitez-Del-Castillo, J.M., Fuchsluger, T., Labetoulle, M., Malachkova, N., Meloni, M., Utheim, T.P., Rolando, M., 2020. Dry eye disease treatment: the role of tear substitutes, their future, and an updated classification. Eur. Rev. Med. Pharmacol. Sci. 17, 8642–8652. https://doi.org/10.26355/eurrev_202009_22801.

Baudouin, C., Messmer, E.M., Aragona, P., Geerling, G., Akova, Y.A., Benítez-del-Castillo, J., Boboridis, K.G., Merayo-Lloves, J., Rolando, M., Labetoulle, M., 2016. Revisiting the vicious circle of dry eye disease: a focus on the pathophysiology of meibomian gland dysfunction. Br. J. Ophthalmol. 3, 300–306. https://doi.org/10.1136/bjophthalmol-2015-307415.

Bron, A.J., de Paiva, C.S., Chauhan, S.K., Bonini, S., Gabison, E.E., Jain, S., Knop, E., Markoulli, M., Ogawa, Y., Perez, V., Uchino, Y., Yokoi, N., Zoukhri, D., Sullivan, D. A., 2017. TFOS DEWS II pathophysiology report. Ocul. Surf. 15 (3), 438–510. https://doi.org/10.1016/j.jtos.2017.05.011.

Carter, R.T., 2009. The role of integrins in corneal wound healing. Vet. Ophthalmol. 12 (1), 2–9. https://doi.org/10.1111/j.1463-5224.2009.00726.x.

Chen, W., Zhang, X., Li, J., Wang, Y., Chen, Q., Hou, C., Garrett, Q., 2013. Efficacy of osmoprotectants on prevention and treatment of murine dry eye. Invest. Ophthalmol. Vis. Sci. 9, 6287–6297. https://doi.org/10.1167/iovs.13-12081.

Craig, J.P., Nelson, J.D., Azar, D.T., Belmonte, C., Bron, A.J., Chauhan, S.K., de Paiva, C. S., Gomes, J.A.P., Hammitt, K.M., Jones, L., Nichols, J.J., Nichols, K.K., Novack, G. D., Stapleton, F.J., Willcox, M.D.P., Wolffsohn, J.S., Sullivan, D.A., 2017. TFOS DEWS II report executive summary. Ocul. Surf. 4, 802–812. https://doi.org/10.1016/j.jtos.2017.08.003.

Draize, J.H., Woodgard, G., Calvery, H.O., 1944. Methods for the study of irritation and toxicity of substances applied topically to the skin and mucous membranes. J. Pharmacol. Exp. Therapeut. 82, 377–390.

Fallacara, A., Baldini, E., Manfredini, S., Vertuani, S., 2018. Hyaluronic acid in the third millennium. Polymers 7, 701. https://doi.org/10.3390/polym10070701.

Garrett, Q., Khandekar, N., Shih, S., Flanagan, J.L., Simmons, P., Vehige, J., Willcox, M. D., 2013. Betaine stabilizes cell volume and protects against apoptosis in human corneal epithelial cells under hyperosmotic stress. Exp. Eye Res. 108, 33–41. https://doi.org/10.1016/j.exer.2012.12.001.

Gomes, J.A., Amankwah, R., Powell-Richards, A., Dua, H.S., 2004. Sodium hyaluronate (hyaluronic acid) promotes migration of human corneal epithelial cells in vitro. Br. J. Ophthalmol. 6, 821–825. https://doi.org/10.1136/bjo.2003.027573.

Gupta, P.K., Asbell, P., Sheppard, J., 2020. Current and future pharmacological therapies for the management of dry eye. Eye Contact Lens 46, S64–S69. https://doi.org/10.1097/ICL.0000000000000666.

Hu, J.W., Zhu, X.P., Pan, S.Y., Yang, H., Xiao, X.H., 2021. Prevalence and risk factors of dry eye disease in young and middle-aged office employee: a Xi'an Study. Int. J. Ophthalmol. 4, 567–573. https://doi.org/10.18240/ijo.2021.04.14.

Kaczara, P., Sarna, T., Burke, J.M., 2010. Dynamics of H_2O_2 availability to ARPE-19 cultures in models of oxidative stress. Free Radic. Biol. Med. 8, 1064–1070. https://doi.org/10.1016/j.freeradbiomed.2010.01.022.

Khare, A., Grover, K., Pawar, P., Singh, I., 2014. Mucoadhesive polymers for enhancing retention in ocular drug delivery: a critical review. Rev. Adhesion Adhes. 4, 467–502. https://doi.org/10.7569/RAA.2014.097310.

Lee Guo, W.O.D., Akpek, E., 2020. The negative effects of dry eye disease on quality of life and visual function. Turk. J. Med. Sci. 7, 1611–1615. https://doi.org/10.3906/sag-2002-143.

Litwiniuk, M., Krejner-Bienias, A., Speyrer, M., Gauto, A., Grzela, T., 2016. Hyaluronic acid in inflammation and tissue regeneration. Wounds 28, 78–88.

Liu, C.Y., Kao, W.W., 2015. Corneal epithelial wound healing. Prog. Mol. Biol. Transl. Sci. 134, 61–71. https://doi.org/10.1016/bs.pmbts.2015.05.002.

Liu, F., Zhang, X., Ling, P., Liao, J., Zhao, M., Mei, L., Shao, H., Jiang, P., Song, Z., Chen, Q., Wang, F., 2017. Immunomodulatory effects of xanthan gum in LPS-stimulated RAW 264.7 macrophages. Carbohydr. Polym. 1 (169), 65–74. https://doi.org/10.1016/j.carbpol.2017.04.003.

Martinotti, S., Ranzato, E., 2020. Scratch wound healing assay. Methods Mol. Biol. 225–229 https://doi.org/10.1007/7651_2019_259.

Maugeri, A., Barchitta, M., Mazzone, M.G., Giuliano, F., Basile, G., Agodi, A., 2018. Resveratrol modulates SIRT1 and DNMT functions and restores LINE-1 methylation levels in ARPE-19 cells under oxidative stress and inflammation. Int. J. Mol. Sci. 7, 2118. https://doi.org/10.3390/ijms19072118.

McDonald, T.O., Shadduck, J.A., 1977. Eye irritation. In: Marzulli, F.N., Maibach, H.I. (Eds.), Advances in Modern Toxicology, Chapter 4. Dermatotoxicology and Pharmacology. John Wiley & Sons, New York, pp. 139–191.

McKay, T.B., Schlötzer-Schrehardt, U., Pal-Ghosh, S., Stepp, M.A., 2020. Integrin: basement membrane adhesion by corneal epithelial and endothelial cells. Exp. Eye Res. 198, 108138 https://doi.org/10.1016/bs.pmbts.2015.05.002.

Menchicchi, B., Fuenzalida, J.P., Hensel, A., Swamy, M.J., David, L., Rochas, C., Goycoolea, F.M., 2015. Biophysical analysis of the molecular interactions between polysaccharides and mucin. Biomacromolecules 3, 924–935. https://doi.org/10.1021/bm501832y.

Nebbioso, M., Del Regno, P., Gharbiya, M., Sacchetti, M., Plateroti, R., Lambiase, A., 2017. Analysis of the pathogenic factors and management of dry eye in ocular surface disorders. Int. J. Mol. Sci. 8, 1764. https://doi.org/10.3390/ijms18081764.

Okumura, Y., Inomata, T., Iwata, N., Sung, J., Fujimoto, K., Fujio, K., Midorikawa-Inomata, A., Miura, M., Akasaki, Y., Murakami, A., 2020. A review of dry eye questionnaires: measuring patient-reported outcomes and health-related quality of life. Diagnostics 8, 559. https://doi.org/10.3390/diagnostics10080559.

Petri, D.F.S., 2015. Xanthan gum: a versatile biopolymer for biomedical and technological applications. J. Appl. Polym. Sci. 132, 42035 https://doi.org/10.1002/app.42035.

Pflugfelder, S.C., Stern, M.E., 2020. Biological functions of tear film. Exp. Eye Res. 197, 108115 https://doi.org/10.1016/j.exer.2020.108115.

Postorino, E.I., Aragona, P., Rania, L., Spinella, R., Puzzolo, D., Micali, A., Mazza, A.M.L., Papa, V., 2020. Changes in conjunctival epithelial cells after treatment with 0.2% xanthan gum eye drops in mild-moderate dry eye. Eur. J. Ophthalmol. 3, 439–445. https://doi.org/10.1177/1120672119833278.

Rolando, M., Barabino, S., 2021. The subtle role of parainflammation in modulating the progression of dry eye disease. Ocul. Immunol. Inflamm. 4, 811–816. https://doi.org/10.1080/09273948.2021.1906908.

Seen, S., Tong, L., 2018. Dry eye disease and oxidative stress. Acta Ophthalmol. 4, e412–e420. https://doi.org/10.1111/aos.13526.

Simmons, P.A., Vehige, J.G., 2017. Investigating the potential benefits of a new artificial tear formulation combining two polymers. Clin. Ophthalmol. 12, 1637–1642. https://doi.org/10.2147/OPTH.S135550.

Smith, J.A., Albenz, J., Begley, C., Caffery, B., Nichols, K., Schaumberg, D., Schein, O., 2007. The epidemiology of dry eye disease: report of the epidemiology subcommittee of the international Dry Eye WorkShop. Ocul. Surf. 5, 93–107. https://doi.org/10.1016/s1542-0124(12)70082-4.

Tsubota, K., Pflugfelder, S.C., Liu, Z., Baudouin, C., Kim, H.M., Messmer, E.M., Kruse, F., Liang, L., Carreno-Galeano, J.T., Rolando, M., Yokoi, N., Kinoshita, S., Dana, R., 2020. Defining dry eye from a clinical perspective. Int. J. Mol. Sci. 23, 9271. https://doi.org/10.3390/ijms21239271.